NANO LETTERS

Letter

pubs.acs.org/NanoLett

Extraordinary Sunlight Absorption and One Nanometer Thick Photovoltaics Using Two-Dimensional Monolayer Materials

Marco Bernardi,[†] Maurizia Palummo,[†,‡] and Jeffrey C. Grossman*[,†]

[†]Department of Materials Science and Engineering, Massachusetts Institute of Technology, 77 Massachusetts Avenue, Cambridge, Massachusetts 02139-4307, United States

[‡]Dipartimento di Fisica, Università di Roma Tor Vergata, CNISM, and European Theoretical Spectroscopy Facility (ETSF), Via della Ricerca Scientifica 1, 00133 Roma, Italy

Supporting Information

ABSTRACT: Graphene and monolayer transition metal dichalcogenides (TMDs) are promising materials for next-generation ultrathin optoelectronic devices. Although visually transparent, graphene is an excellent sunlight absorber, achieving 2.3% visible light absorbance in just 3.3 Å thickness. TMD monolayers also hold potential as sunlight absorbers, and may enable ultrathin photovoltaic (PV) devices due to their semiconducting character. In this work, we show that the three TMD monolayers MoS_2, $MoSe_2$, and WS_2 can absorb up to 5−10% incident sunlight in a thickness of less than 1 nm, thus achieving 1 order of magnitude higher sunlight absorption than GaAs and Si. We further study PV devices based on just two stacked monolayers: (1) a Schottky barrier solar cell between MoS_2 and graphene and (2) an excitonic solar cell based on a MoS_2/WS_2 bilayer. We demonstrate that such 1 nm thick active layers can attain power conversion efficiencies of up to ∼1%, corresponding to approximately 1−3 orders of magnitude higher power densities than the best existing ultrathin solar cells. Our work shows that two-dimensional monolayer materials hold yet untapped potential for solar energy absorption and conversion at the nanoscale.

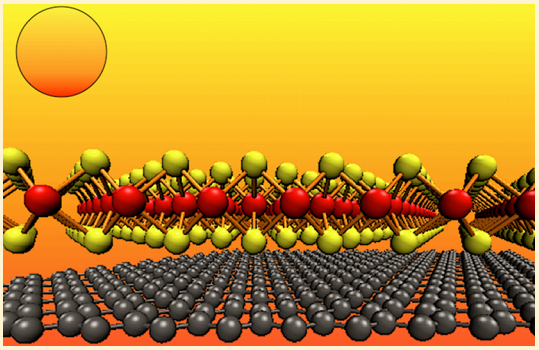

KEYWORDS: *Monolayer materials, graphene, transition metal dichalcogenides, solar energy, sunlight absorption, photovoltaics*

Following the pioneering work from Geim and colleagues showing the mechanical exfoliation of graphene with the scotch tape method,[1] monolayers of BN,[2] hybrid graphene-BN,[3] MoS_2,[4,5] $MoSe_2$,[6] and WS_2[7] have been prepared by exfoliation and chemical vapor deposition. While technical barriers toward large-scale synthesis of monolayer materials continue to be overcome, studies of micrometer-scale flakes complemented by theoretical calculations have already highlighted a host of novel optical and electronic properties in these materials.[8−11] For example, the three transition metal dichalcogenides (TMDs) MoS_2, $MoSe_2$, and WS_2 undergo a crossover from indirect to direct gap when going from bilayer to monolayer,[12] resulting in enhanced monolayer photoluminescence.[6,7,13] Although graphene has been used in optoelectronics and photovoltaics (PV) as a transparent contact, it displays an extraordinary absorbance of 2.3% in the visible considering its thickness of only 3.3 Å.[14] Such an absorbance is equivalent to that of approximately 20 nm thick Si or 5 nm thick GaAs, namely, two of the most commonly used absorbers in solar cells.[15] This high optical absorption of graphene and other two-dimensional monolayers makes such materials appealing for solar energy conversion.[16,17] Although it may appear counterintuitive to use graphene as a key active material in PV given its transparency and metallic behavior, the idea of coupling a semiconducting TMD monolayer with graphene to create a bilayer Schottky barrier solar cell is viable. In addition, solar cell active layers obtained by stacking two different TMD monolayers are also possible. The high carrier mobility of monolayer materials, including values of over 200 000 $cm^2/V{\cdot}s$ for suspended graphene[8] and up to 200 $cm^2/V{\cdot}s$ in monolayer MoS_2,[4] also make them appealing for PV applications. Such high mobilities coupled to the possibility of making ultrathin solar cells can lead to monolayer-based PV with very low series resistance, large voltages, and near-optimal $I-V$ curves.

Here we study the feasibility and predict the performance of 1 nm thick solar cells based on bilayers of MoS_2/graphene or two stacked TMD monolayers. First, we use a combination of first principles calculations based on density functional theory (DFT) and the GW-Bethe Salpeter method[18−20] to compute accurate absorbance spectra for monolayers of MoS_2, $MoSe_2$, WS_2, and graphene, showing quantitative agreement with available experimental measurements for MoS_2 and graphene. Our calculations show that a *single TMD monolayer* with subnanometer thickness can absorb as much sunlight as 50 nm of Si and generate electrical currents as high as 4.5 mA/cm^2.

Received: April 27, 2013
Revised: June 5, 2013
Published: June 10, 2013

Next, we compute the band alignment in bilayers of MoS_2/graphene and MoS_2/WS_2 and demonstrate that both these interfaces can realize PV operation by formation of a Schottky barrier and a type-II heterojunction, respectively. Using conservative assumptions, we compute that such bilayer solar cells can reach over 1% power conversion efficiency (PCE) in just 1 nm thickness, thus packing a power density of up to 2.5 MW/kg, a value that is far superior to any known energy conversion or storage device. These calculations illustrate new avenues for nanoscale solar energy conversion using TMD monolayers and graphene.

Accurate computation of optical absorption in TMD monolayers (Figure 1a) is challenging due to a number of technical reasons. In this work, we employ DFT calculations, the GW method,[19] and the Bethe–Salpeter equation (BSE)[20] to obtain the macroscopic dielectric tensor including an accurate account of electron–electron and electron–hole interactions, as well as spin–orbit and semicore state effects. The calculations were carried out using the VASP[21,22] and Yambo[23] codes and are detailed in the Supporting Information.

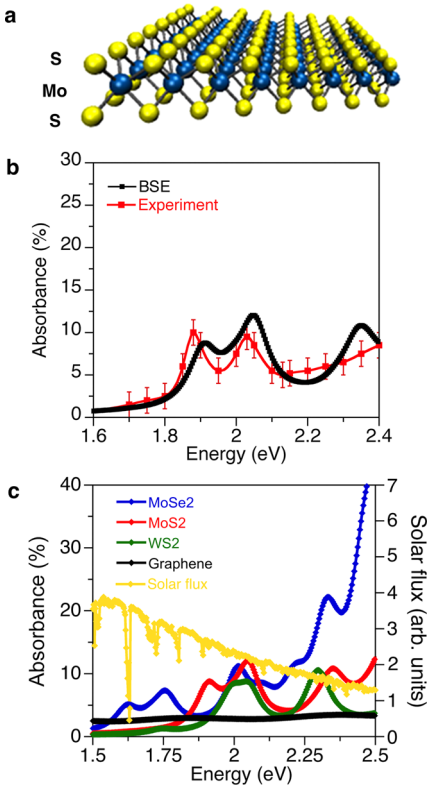

Figure 1. Absorbance of TMD monolayers. (a) Schematic drawing of the MoS_2 monolayer structure used in this work. The yellow spheres represent S atoms and the blue spheres Mo atoms. (b) Comparison of the computed and experimental absorbance of monolayer MoS_2. The error bars in the experimental curve were taken with an absolute value of ±1.5% due to the presence of a nonzero baseline in the spectrum in ref 12. (c) Absorbance of three TMD monolayers and graphene, overlapped to the incident AM1.5G solar flux.

Figure 1b compares our computed absorbance for a monolayer of MoS_2 with the experimental measurements of Mak et al.[12] The quantitative agreement observed between the computed and experimental absorbance highlights the accuracy of our approach. Figure 1c shows the absorbance calculated for the three TMD monolayers MoS_2, $MoSe_2$, and WS_2, compared to the absorbance of graphene (as computed here, in good agreement with the flat 2.3% value measured by Nair et al.[14]) and to the incident AM1.5G solar spectrum.[24] We predict that TMD monolayers possess a high absorbance of 5–10% in the visible, and can thus capture a significant fraction of incident sunlight in a subnanometer thickness. Table 1 compares the absorbed photon flux J_{abs} in graphene, the three TMD monolayers studied here, and 1 nm thick layers of materials commonly used in thin-film inorganic (Si and GaAs) and organic (P3HT polymer) solar cells, whose bulk absorption spectrum was taken from experimental data in the literature.

Table 1. Absorbed Photon Flux J_{abs} under AM1.5G Solar Illumination for Graphene and TMD Monolayers, Computed Using Equation 1 with the Absorbance Values in Figure 1c[a]

material	E_g (eV) at 300 K	J_{abs} (mA/cm^2)
graphene	0.0	2.0
MoS_2	1.89[12]	3.9
$MoSe_2$	1.64[6]	4.6
WS_2	1.96[7]	2.3
Si	1.11[15]	0.1
GaAs	1.42[15]	0.3
P3HT	1.95[25]	0.2

[a] J_{abs} quantifies the flux of absorbed photons, converted to units of equivalent electrical current. The optical gap of each material is also shown (taken from the literature, as referenced in the table). The same quantities are shown for 1 nm thick representative bulk materials of relevance in ultrathin PV, whose absorption coefficient α was taken from the literature (see refs in the table) and converted to absorbance for a flat layer of thickness L = 1 nm using $A = 1 - \exp(-\alpha L)$.

For each material, J_{abs} is calculated using the absorbance A from the integral:

$$J_{abs} = e \int_{E_g}^{\infty} A(E) J_{ph}(E)\, dE \quad (1)$$

where E_g is the optical gap of the absorber, $J_{ph}(E)$ is the incident photon flux (units of photons/cm^2·s·eV), and E is the photon energy. By multiplying by the elementary charge e, the absorbed photon flux is expressed as the equivalent short-circuit electrical current density (units of mA/cm^2) in the ideal case when every photon is converted to a carrier extracted in a PV device, so that J_{abs} sets the upper limit for the contribution of the single material to the solar cell short-circuit current. We remark that this choice of units represents nothing more than a convenient way to quantify sunlight absorption and is fully equivalent to expressing the results in terms of the absorbed photon flux.

Our results indicate that subnanometer thick graphene and TMD monolayers can absorb photon fluxes equivalent to short-circuit currents of 2–4.5 mA/cm^2, while 1 nm thick Si, GaAs, and P3HT all generate currents in the 0.1–0.3 mA/cm^2 range. For example, approximately 15 nm of GaAs or 50 nm of Si are needed to absorb the same fraction of sunlight as a TMD monolayer such as $MoSe_2$. While the absorbance of graphene is regulated by the fine structure constant,[14] we discuss here the origin of the large absorbance in TMD monolayers. The valence and conduction bands energetically close to the gap in TMD monolayers are dominated by localized d states of the transition metal atoms.[13,26] Within an independent-particle treatment, the high optical absorption at visible energies in

dx.doi.org/10.1021/nl401544y | Nano Lett. 2013, 13, 3664–3670

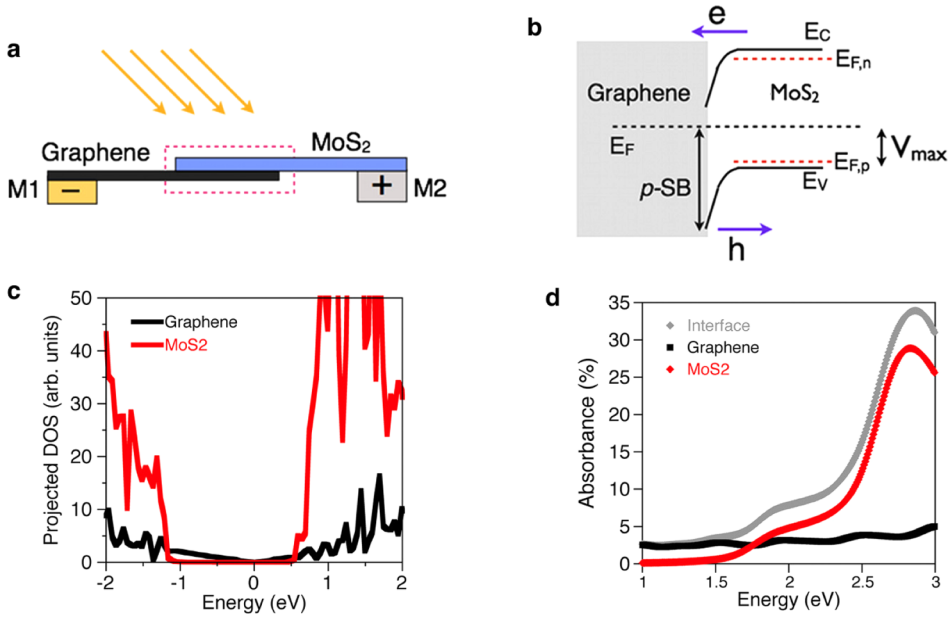

Figure 2. MoS_2/graphene interface and Schottky barrier solar cell. (a) The MoS_2/graphene solar cell described in this work. M1 and M2 are, respectively, low and high workfunction metals. The MoS_2/graphene junction is shown enclosed in a dashed box. The polarity of the electrodes is also shown. (b) Band alignment at a MoS_2/graphene interface, as predicted using DFT. *p*-SB is the hole Schottky barrier; also shown are the valence and conduction band edges (E_v and E_c, respectively) of MoS_2 as well as the quasi-Fermi levels for electrons and holes under illumination ($E_{F,n}$ and $E_{F,p}$, shown as red dashed lines), together with the direction of electron and hole diffusion. V_{max} is the maximum open-circuit voltage. (c) PDOS of a MoS_2/graphene interface. The energy is referenced to the Fermi energy. (d) Absorbance of the MoS_2/graphene interface and its composing monolayers, computed within the independent particle approximation using DFT.

TMD monolayers can be explained by dipole transitions with large joint density of states and oscillator strengths between localized *d* states with strong spatial overlap; such transitions are dipole-allowed in a regime of weak spin−orbit coupling, as exhibited by MoS_2 and other TMD systems. This observation that a major role is played by strong dipole transitions between localized *d* states is supported by recent work of Britnell et al.,[27] although we note that such an independent-particle picture is only partially complete. In particular, excitonic effects in TMD monolayers[28] resulting from the poor screening of electrons and holes due to the vacuum surrounding the monolayer, give rise to a strong mixing of electron−hole configurations in the excited-state wave function. This results in a constructive superposition of the oscillator strengths for transitions at low energies near the absorption onset, as also found in other semiconductors.[29] To quantify the different contributions giving rise to the large optical absorption at visible energies for the case of MoS_2, we compare two different approaches for computing the absorbance in Figure S1: the independent-particle absorbance computed using DFT with the random phase approximation (DFT-RPA) which includes only dipole transitions, and the absorbance shown in Figure 2b obtained using BSE which explicitly includes electron−hole interactions. As shown in Figure S1, excitonic effects increase the absorbance at visible energies by a factor of ∼2 compared to DFT-RPA. This result suggests that, while part of the reason for the strong absorption in monolayer MoS_2 is due to the dipole transition between localized *d* orbitals contributing to visible absorbances in the 2−5% range, another important contribution arises from excitonic coupling of such transitions and is responsible for increasing the absorbance further up to 5−10%. A similar behavior is found for the other TMD monolayers studied in this work.

It is important to compare the absorption in graphene and TMD monolayers with those of their bulk counterparts—respectively, graphite and bulk TMDs—composed by stacked multilayers held together by van der Waals forces. We focus in this comparison on visible photon energies in the 1−2.5 eV range of key relevance for photovoltaics, and for TMD monolayers analyze the case of MoS_2, for which accurate absorption experiments are available for the bulk. Monolayer MoS_2 has an absorbance of $A \approx 5-10\%$ in a thickness $\Delta z = 6.5$ Å. Although strictly speaking one cannot define a macroscopic absorption coefficient in the layer-normal direction for a single layer of MoS_2 (since by definition this quantity should be averaged over several unit cells of the material), the equivalent absorption coefficient α for monolayer MoS_2 can be obtained as $\alpha = A/\Delta z = 1-1.5 \times 10^6$ cm^{-1}. Similar values are found for the case of graphene ($A = 2.3\%$, $\Delta z = 3.3$ Å, and thus $\alpha = 0.7 \times 10^6$ cm^{-1}). These absorption coefficients are higher than those found in bulk MoS_2[30] and graphite[31] at visible energies of up to 2.5 eV: for bulk MoS_2, experimental measurements suggest α values in the $0.1-0.6 \times 10^6$ cm^{-1} range,[30] while for graphite experiments suggest α values of $0.2-0.4 \times 10^6$ cm^{-1} (see ref 31). The absorption values are thus higher by a factor of 2−3 for both graphene and MoS_2 monolayers compared to their bulk counterparts. To allow a direct comparison of monolayer and bulk MoS_2 with our calculation approach, we computed the absorption coefficient of bulk MoS_2 using BSE (see Figure S2 in Supporting Information) and find excellent agreement with the experimental absorption values of $0.1-0.6 \times 10^6$ cm^{-1} in ref 30. Experimental measurements for bulk GaAs—which is used here as a reference material with high visible absorption—also show α values in the 10^4-10^5 cm^{-1} range.[15] We note that, despite the linear scaling in absorbance versus number of layers for up to 4−5 layers of MoS_2 and graphene, the different values of optical absorption in the bulk versus monolayer forms

dx.doi.org/10.1021/nl401544y | *Nano Lett.* 2013, 13, 3664−3670

Table 2. Comparison between the Performance of Record Ultrathin Solar Cells Based on Si and GaAs and the MoS_2/Graphene and Bilayer TMD Solar Cells Studied Here[a]

material	thickness	efficiency	weight (g/m^2)	power density (kW/L)	power density (kW/kg)
GaAs	1 μm	~29%[38]	5.3	290	54
Si	35 μm	20.6%[39]	92.7	5.9	2.5
graphene/MoS_2	0.9 nm	0.1−1.0%	3.9×10^{-3}	1000−10 000	250−2500
WS_2/MoS_2	1.2 nm	0.4−1.5%	7.9×10^{-3}	3000−12 000	450−1800

[a]Thickness and weight refer solely to the device active layer. Efficiency is the PCE under AM1.5G illumination.

suggest that after stacking a sufficiently high number of layers a "bulk-like" behavior emerges. For graphene, deviation from this linear dependence of absorbance versus number of layers has been observed beyond 4−5 layers,[14] while for TMD this linear dependence has been shown only for up to 3−4 layers.[12] We suggest that further work is necessary to establish the difference and the transition between monolayer and bulk behavior in layered materials.

The exceptional sunlight absorption of graphene and TMD monolayers discussed so far suggests the possibility to design 1-nm-thick solar cells based on just two stacked monolayers, a topic we develop in the remainder of the paper. The first device we examine is based on a bilayer of MoS_2/graphene as the active layer material. Figure 2a shows a possible geometry for a solar cell formed using a bilayer of MoS_2/graphene interfaced to a high workfunction metal on the MoS_2 side and a low workfunction metal on the graphene side. Since graphene is a (semi)metal and MoS_2 is a semiconductor, in order for such a device to work electron−hole pairs generated in either material composing the interface should be separated through the formation of a Schottky barrier (SB). We employ DFT combined with the lineup method[32] to study the formation of a SB at an interface between graphene and a defect-free, undoped layer of MoS_2 (see Supporting Information). The first step in this calculation is the determination of the work functions of MoS_2 and graphene. Using DFT, we computed a workfunction value of $\phi_{MoS_2} = 5.2$ eV for monolayer MoS_2, in agreement with the recent experimental observation of ohmic contact between *n*-type MoS_2 and Au,[4] and a workfunction of $\phi_G = 4.25$ eV for graphene, which is close to commonly measured values in the 4.3−4.6 eV range. Our calculations further predict the formation of a SB of 1.2 eV for holes to diffuse from graphene to MoS_2, thus enabling the design of SB solar cells between (preferably *p*-type) MoS_2 and graphene. Charge separation occurs by injecting photogenerated electrons from the conduction band of MoS_2 to graphene, while holes photogenerated in the valence band of MoS_2 cannot diffuse to graphene due to the large SB (see Figure 2b). Notably, electron injection from MoS_2 to graphene upon illumination as predicted here has been observed by recent experiments in MoS_2/graphene phototransistors.[33] Under these operating conditions, the maximum open circuit voltage $V_{OC,max}$ is set by the difference between the SB and the built-in potential, given that holes are extracted at the VBM in MoS_2 (namely, the maximum quasi-Fermi hole level that can be reached under illumination). We estimate a relatively small $V_{OC,max} \approx 0.3$ eV, obtained as the difference between the computed SB of 1.2 eV and the built-in potential $\phi_{MoS_2} - \phi_G \approx 0.9$ eV.[34]

We remark that our calculation assumes that the metallic electrode contacting the MoS_2 monolayer is placed sufficiently far (i.e., at least one screening length away) from the MoS_2/graphene junction (Figure 2a), so that the Fermi energy near the contact recovers its value in monolayer MoS_2 unaffected by the interface dipole induced by graphene. This assumption justifies the alignment shown in Figure 2b, where band bending in MoS_2 occurs in a direction parallel to the monolayer when moving away from the junction area toward the electrode contacting MoS_2. Our proposed geometry with the electrodes spatially separated from the junction further reduces the risk of leakage currents potentially occurring if the bilayer solar cell is placed between two metallic electrodes separated by just 1 nm. While our calculations suggest that a *p*-type doping is preferable in MoS_2, some experiments have shown that MoS_2 deposited on SiO_2 shows *n*-type behavior.[4] However, recent calculations suggest that the doping type in MoS_2 may not be intrinsic but rather due to impurities or defects at the SiO_2 surface,[35] as further supported by experiments reporting *p*-type behavior in MoS_2.[35]

Figure 2c−d shows other important aspects of the MoS_2/graphene bilayer proposed here. Upon formation of the interface, our calculations suggest a redistribution of the ground state charge in the system, as also concluded in a recent study by Ma et al.[36] Despite this effect, the projected density of states (PDOS) shows that the electronic states of graphene and MoS_2 do not hybridize near the Fermi energy (Figure 2c). In addition, the absorbance at visible photon energies (computed here using DFT within the independent particle approximation[20] due to the large size of the simulation cell) is equal to the sum of the absorbances of isolated graphene and the MoS_2 monolayer (Figure 2d). Using the absorbance spectrum in Figure 2d and eq 1, we estimate a maximum short-circuit current of $J_{abs} = 4.3$ mA/cm^2 for a MoS_2/graphene active layer. This value differs slightly from the sum of the monolayer currents in Table 1 (5.9 mA/cm^2) due to the use of different levels of theory (BSE in Table 1 and independent-particle in Figure 2d); for our purpose here it suffices to establish that a maximum short-circuit current of ~4.5 mA/cm^2 can be achieved. We estimate a range of PCE values for the MoS_2/graphene solar cell in Figure 2a by using $J_{abs} = 4.5$ mA/cm^2 combined with: (1) for the lower PCE limit, an open circuit voltage $V_{OC} = 0.1$ V and a small fill factor (FF) of 0.3, namely, a reasonable value for a "poor" solar cell device with high series and low shunt resistances, and (2) for the upper PCE limit, $V_{OC} = 0.5$ V and FF = 0.6 as a reasonable FF value in a device with effective carrier transport.[37] In all cases, a conservative value of 0.7 is assumed for the internal quantum efficiency (IQE, namely the fraction of absorbed photons extracted as carriers at the contacts), a value significantly lower than the best Si and GaAs solar cells achieving IQE close to unity. This approach corresponds to assuming that only 70% of the absorbed photons contribute to the current, resulting in a short-circuit current $J_{SC} = 0.7 \cdot J_{abs}$ in the solar cell device. We compute the PCE under AM1.5G illumination by dividing the product $J_{SC} \times V_{OC} \times$ FF through the incident power of 100 mW/cm^2,[37] resulting in a PCE range of 0.1−1.0% for a bilayer of MoS_2/

dx.doi.org/10.1021/nl401544y | Nano Lett. 2013, 13, 3664−3670

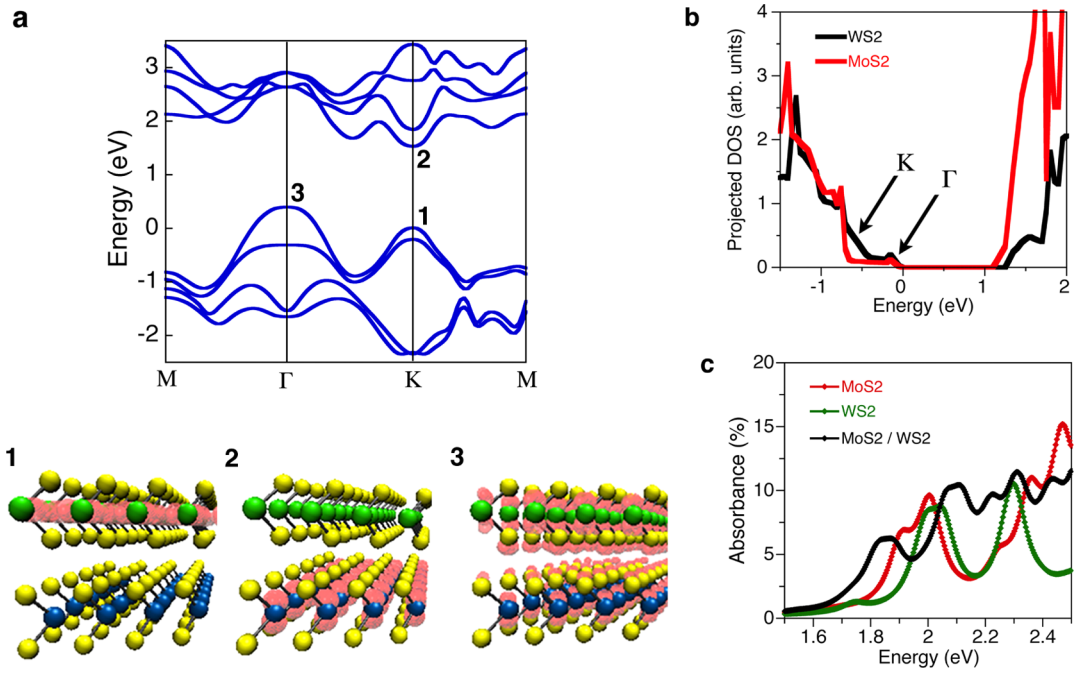

Figure 3. MoS_2/WS_2 interface and excitonic solar cell. (a) DFT bandstructure of the MoS_2/WS_2 bilayer. Shown in red below the plot is the charge density associated with the wave functions for the $\vec{k}$-points and bands marked as 1−3. At the K point, the VBM stems from states in WS_2 and the CBM from states in MoS_2, while the VBM at Γ shows contributions from both layers. The atoms are shown as yellow (S), blue (Mo), and green (W) spheres. (b) PDOS of the MoS_2/WS_2 bilayer, showing type-II alignment consistent with the charge density plots shown in a. The energy is referenced to the Fermi energy, and the arrows indicate PDOS features in the VBM due, respectively, to electronic states at the K and Γ points of the Brillouin zone. (c) Absorbance spectra of the MoS_2/WS_2 bilayer and of the individual composing layers, computed using BSE.

graphene. Despite the relatively low efficiency compared to thicker active layers, the power generated by a unit volume or mass of active layer material (power density) in a 1% efficient MoS_2/graphene solar cell would be incredibly high. Table 2 compares the power density of a MoS_2/graphene solar cell to the power densities of ultrathin solar cells based on GaAs[38] and Si[39] with current records of thickness and efficiency. We estimate that a MoS_2/graphene bilayer with a thickness of 0.9 nm, a weight of 3.9 mg/m^2, and an efficiency of 0.1−1.0% as derived above would achieve a power density of 1.0−10.0 MW/L or 0.25−2.5 MW/kg. Such values are higher by approximately 1−3 orders of magnitude compared to existing record solar cells, and higher than any known energy generation and conversion device.[40,41] We remark that, although power density is not a conventional figure of merit in PV, it is an important metric to understand the ultimate power generation limits in solar cells achieving the smallest possible thickness, as well as to estimate the energy achievable from a unit volume or weight of active layer material.[42] For example, Table 2 indicates that a 1% efficient solar cell based on MoS_2/graphene is 30 times less efficient than the best 1 μm thick device based on GaAs, but using a thickness 1000 times smaller; this corresponds to a generated power per unit volume (or equivalently, per unit thickness) higher by a factor of ∼30 for MoS_2/graphene compared to GaAs.

We highlight the fact that the PCE (and thus power density) values estimated here for a MoS_2/graphene solar cell are well-grounded: the absorbed photon flux J_{opt} is estimated from accurate calculations of the absorbance closely matching experimental results (Figure 1b), the chosen V_{OC} values are moderate (0.1−0.5 V) and within the range estimated above using DFT, and a realistic range of FF values[37] of 0.3−0.6 as well as a moderate IQE value of 0.7 were assumed in our calculations. Rather conservative values have been chosen for all the quantities composing the PCE, and the high power densities obtained are the sole consequence of the high absorbance for very small thickness in graphene and TMD monolayers.

We next estimate the feasibility and performance of another possibility for 1-nm-thick PV, this time constituted by an interface between the two semiconducting monolayers MoS_2 and WS_2, which would need to form a type-II heterojunction to enable exciton dissociation and charge separation.[17] Different from the MoS_2/graphene interface, the interaction between two TMD monolayers leads to significant changes in the bandstructure and absorption spectrum compared to the isolated monolayers. In particular, the DFT bandstructure of the MoS_2/WS_2 interface shows the formation of an indirect gap due to the interaction of antibonding p_z orbitals from S atoms in the two TMD monolayers, resulting in an increase of the VBM energy at Γ (Figure 3a). The VBM at K shows contributions only from in-plane d orbitals of WS_2, while the CBM at K is contributed only by d_{z^2} orbitals of MoS_2; this set of orbital contributions to the electronic states is common in TMD systems.[26] The band gap at the K point is typically responsible for the photoabsorption onset at visible energies in TMD systems. In the present case, the nature of the electronic states at the K point implies that the absorption of a photon with visible energy transfers an electron from a state localized on MoS_2 to a state localized on WS_2, thus achieving the formation of a charge-transfer exciton shared by the two layers. Consistent with this picture, a type-II alignment favorable for solar cell operation is achieved at the MoS_2/WS_2 interface, where WS_2 behaves as the donor and MoS_2 as the acceptor, as shown by the analysis of the PDOS in Figure 3b.[43] Although the VBM states near the Γ point are an exception as they stem

dx.doi.org/10.1021/nl401544y | Nano Lett. 2013, 13, 3664−3670

from both monolayers and may act as recombination centers, we expect the key photoexcitation at visible photon energies to involve states at the K point and thus conclude that the observed band alignment would lead to effective PV operation. Owing to the interlayer interaction leading to the formation of an indirect gap, the optical absorption spectrum of the bilayer obtained from BSE shows significant differences from the sum of the spectra of the two composing layers (Figure 3c). In particular, the bilayer absorbance is lower than the sum of the absorbances of the individual layers, and the absorption spectrum shows the formation of a lower absorption edge compared to the composing layers, thus confirming the presence of charge-transfer excitons. Using eq 1, we estimate a maximum short circuit current $J_{opt} \approx 3.5$ mA/cm^2 for the MoS_2/WS_2 bilayer (close to the value for isolated MoS_2), and we extract from the PDOS a maximum open circuit voltage of ~1 V, equal to the band gap of the type-II interface (see Figure 3b). Using an IQE value of 0.7, FF values in the 0.3−0.6 range as above, and a V_{OC} of 0.5−1 V, we estimate PCE values of 0.4−1.5% for a bilayer of MoS_2/WS_2 with a 1.2 nm thickness and a weight of only 7.9 mg/cm^2, resulting in ultrahigh power densities similar to the MoS_2/graphene case (see Table 2).

The PV efficiencies computed here could be increased using a number of strategies in a real device. For example, an increase by a factor of 2 in the efficiency compared to what is estimated here can be gained using a double pass of light in the active layer, as can be obtained by employing a back metallic contact in the absence of light interference effects. In addition, since the absorbance of graphene and MoS_2 has been measured to double and triple, respectively, for a bilayer and trilayer,[12,14] a stacking of three graphene monolayers and three MoS_2 monolayers with a back metallic contact may afford maximum efficiencies close to 10% in a 3 nm thick active layer. A similar configuration would require that a SB can be formed at a trilayer graphene/trilayer MoS_2 interface, a point worthy of additional investigation. We further suggest that given the variability of band gaps observed in TMD monolayers, usually in the 1.5−2.5 eV range and decreasing for increasing sizes of the chalcogen atom, significant band gap engineering is possible using stacked TMD bilayers and multilayers. This scenario entails novel possibilities to form broadband sunlight absorbers and enhance efficiencies considerably beyond the values estimated here. Finally, since MoS_2 can catalyze water splitting,[44,45] the excellent sunlight absorption properties predicted here for TMD monolayers could also be employed in the photoelectrochemical generation of hydrogen. In conclusion, our calculations unveil the potential of graphene and TMD monolayers for solar energy absorption and conversion at the nanometer scale.

■ ASSOCIATED CONTENT

Ⓢ Supporting Information

Methods: Details of the DFT, GW, and BSE calculations. Figure S1: Comparison of independent-particle and BSE absorption spectra of monolayer MoS_2. Figure S2: Absorption coefficient of bulk MoS_2. This material is available free of charge via the Internet at http://pubs.acs.org.

■ AUTHOR INFORMATION

Corresponding Author

*E-mail: jcg@mit.edu.

Notes

The authors declare no competing financial interest.

■ ACKNOWLEDGMENTS

M.B. acknowledges fruitful discussions with Dr. David Strubbe and Dr. Can Ataca. M.P. thanks Dr. Ludger Wirtz for sharing his insight on the role of semicore electrons in GW calculations of TMD monolayers. The authors thank NERSC and XSEDE for providing computational resources. M.P. thanks CINECA for providing computational resources through the ISCRA-C project no. HP10CMAA6K. M.P. acknowledges financial support from FP7 ITN "Clermont4" (235114). The authors acknowledge financial support from a MITEI Seed Fund and the MISTI program.

■ REFERENCES

(1) Novoselov, K.; Geim, A.; Morozov, S.; Jiang, D.; Zhang, Y.; Dubonos, S.; Grigorieva, I.; Firsov, A. *Science* **2004**, *306*, 666−669.
(2) Kim, K. K.; Hsu, A.; Jia, X.; Kim, S. M.; Shi, Y.; Hofmann, M.; Nezich, D.; Rodriguez-Nieva, J. F.; Dresselhaus, M.; Palacios, T.; Kong, J. *Nano Lett.* **2012**, *12*, 161−166.
(3) Ci, L.; Song, L.; Jin, C.; Jariwala, D.; Wu, D.; Li, Y.; Srivastava, A.; Wang, Z.; Storr, K.; Balicas, L.; Liu, F.; Ajayan, P. M. *Nat. Mater.* **2010**, *9*, 430−435.
(4) Radisavljevic, B.; Radenovic, A.; Brivio, J.; Giacometti, V.; Kis, A. *Nat. Nanotechnol.* **2011**, *6*, 147−150.
(5) Lee, Y.-H.; Zhang, X.-Q.; Zhang, W.; Chang, M.-T.; Lin, C.-T.; Chang, K.-D.; Yu, Y.-C.; Wang, J. T.-W.; Chang, C.-S.; Li, L.-J.; Lin, T.-W. *Adv. Mater.* **2012**, *24*, 2320−2325.
(6) Tongay, S.; Zhou, J.; Ataca, C.; Lo, K.; Matthews, T. S.; Li, J.; Grossman, J. C.; Wu, J. *Nano Lett.* **2012**, *12*, 5576−5580.
(7) Gutierrez, H. R.; Perea-Lopez, N.; Elias, A. L.; Berkdemir, A.; Wang, B.; Lv, R.; Lopez-Urias, F.; Crespi, V. H.; Terrones, H.; Terrones, M. *Nano Lett.* **2012**, DOI: 10.1021/nl3026357.
(8) Geim, A. K. *Science* **2009**, *324*, 1530−1534.
(9) Castro Neto, A. H.; Guinea, F.; Peres, N. M. R.; Novoselov, K. S.; Geim, A. K. *Rev. Mod. Phys.* **2009**, *81*, 109−162.
(10) Novoselov, K. S.; Jiang, D.; Schedin, F.; Booth, T. J.; Khotkevich, V. V.; Morozov, S. V.; Geim, A. K. *Proc. Natl. Acad. Sci. U.S.A.* **2005**, *102*, 10451−10453.
(11) Ataca, C.; Sahin, H.; Ciraci, S. *J. Phys. Chem. C* **2012**, *116*, 8983−8999.
(12) Mak, K. F.; Lee, C.; Hone, J.; Shan, J.; Heinz, T. F. *Phys. Rev. Lett.* **2010**, *105*, 136805.
(13) Splendiani, A.; Sun, L.; Zhang, Y.; Li, T.; Kim, J.; Chim, C.-Y.; Galli, G.; Wang, F. *Nano Lett.* **2010**, *10*, 1271−1275.
(14) Nair, R. R.; Blake, P.; Grigorenko, A. N.; Novoselov, K. S.; Booth, T. J.; Stauber, T.; Peres, N. M. R.; Geim, A. K. *Science* **2008**, *320*, 1308.
(15) Palik, E. D. *Handbook of Optical Constants of Solids*; Academic Press: New York, 1998; Vol. 3.
(16) Ginley, D.; Green, M. A.; Collins, R. *MRS Bull.* **2008**, *33*, 355−364.
(17) Gregg, B. A. *MRS Bull.* **2005**, *30*, 20−22.
(18) Martin, R. M. *Electronic Structrure: Basic Theory and Practical Methods*; Cambridge University Press: New York, 2008.
(19) Hybertsen, M. S.; Louie, S. G. *Phys. Rev. B* **1986**, *34*, 5390−5413.
(20) Onida, G.; Reining, L.; Rubio, A. *Rev. Mod. Phys.* **2002**, *74*, 601−659.
(21) Kresse, G.; Furthmüller, J. *Phys. Rev. B* **1996**, *54*, 11169.
(22) Shishkin, M.; Kresse, G. *Phys. Rev. B* **2006**, *74*, 035101.
(23) Marini, A.; Hogan, C.; Gruning, M.; Varsano, D. *Comput. Phys. Commun.* **2009**, *180*, 1392−1403.
(24) The AM1.5G spectrum was taken from the NREL website: http://rredc.nrel.gov/solar/spectra/am1.5 and integrated with the trapezoid rule.

(25) Brown, P. J.; Thomas, D. S.; Köhler, A.; Wilson, J. S.; Kim, J.-S.; Ramsdale, C. M.; Sirringhaus, H.; Friend, R. H. *Phys. Rev. B* **2003**, *67*, 064203.
(26) Coehoorn, R.; Haas, C.; De Groot, R. *Phys. Rev. B* **1987**, *35*, 6203.
(27) Britnell, L.; Ribeiro, R. M.; Eckmann, A.; Jalil, R.; Belle, B. D.; Mishchenko, A.; Kim, Y.-J.; Gorbachev, R. V.; Georgiou, T.; Morozov, S. V.; Grigorenko, A. N.; Geim, A. K.; Casiraghi, C.; Neto, A. H. C.; Novoselov, K. S. *Science* **2013**, DOI: 10.1126/science.1235547.
(28) Ramasubramaniam, A. *Phys. Rev. B* **2012**, *86*, 115409.
(29) Rohlfing, M.; Louie, S. G. *Phys. Rev. Lett.* **1998**, *81*, 2312−2315.
(30) Beal, A.; Hughes, H. *J. Phys. C: Solid State Phys.* **1979**, *12*, 881−890.
(31) Taft, E. A.; Philipp, H. R. *Phys. Rev.* **1965**, *138*, A197 The absorption coefficient α of graphite was obtained from the optical conductivity σ in Figure 6 using $\alpha = (4\pi/(c{\cdot}n))\sigma$, where $n \approx 2.2$ is the refractive index of graphite..
(32) Shan, B.; Cho, K. *Phys. Rev. B* **2004**, *70*, 233405.
(33) Zhang, W.; Chuu, C.-P.; Huang, J.-K.; Chen, C.-H.; Tsai, M.-L.; Chang, Y.-H.; Liang, C.-T.; He, H., Jr.; Chou, M.-Y.; Li, L.-J. *ArXiv e-prints* **2013**, arXiv:1302.1230.
(34) We remark that this result is prone to variations in a real device depending on Fermi-level pinning at the MoS_2/metal interface and on device processing conditions, so that a quantitatively accurate limit of the open-circuit voltage can only be predicted when all such variables are defined.
(35) Dolui, K.; Rungger, I.; Sanvito, S. *ArXiv e-prints* **2013**, arXiv:1301.2491.
(36) Ma, Y.; Dai, Y.; Guo, M.; Niu, C.; Huang, B. *Nanoscale* **2011**, *3*, 3883−3887.
(37) Lunt, R. R.; Osedach, T. P.; Brown, P. R.; Rowehl, J. A.; Bulović, V. *Adv. Mater.* **2011**, *23*, 5712−5727.
(38) Miller, O. D.; Yablonovitch, E.; Kurtz, S. R. *IEEE J. Photovoltaics* **2012**, *2*, 303−311; see also http://www.altadevices.com.
(39) See http://www.solexel.com and http://www.appliednanotech.net/news/130103_Solexel_Achievement.php.
(40) Ginley, D. S.; Cahen, D. *Fundamentals of materials for energy and environmental sustainability*; Cambridge University Press: New York, 2011.
(41) Smil, V. *Energy*; Oneworld: London, 2001.
(42) Kaltenbrunner, M.; White, M. S.; Głowacki, E. D.; Sekitani, T.; Someya, T.; Sariciftci, N. S.; Bauer, S. *Nat. Commun.* **2012**, *3*, 770.
(43) We note that, although the band alignment is inferred here from a DFT calculation, the type-II alignment is retained both at the GW and BSE levels of theory and the BSE optical gaps are numerically close to the DFT gaps due to a compensation of errors at the DFT level. This situation is also found in other monolayer systems. Hence, correcting the DFT gaps to the GW or BSE gaps would not change the type-II alignment for the MoS_2/WS_2 interface.
(44) Jaramillo, T. F.; Jørgensen, K. P.; Bonde, J.; Nielsen, J. H.; Horch, S.; Chorkendorff, I. *Science* **2007**, *317*, 100−102.
(45) Kibsgaard, J.; Chen, Z.; Reinecke, B. N.; Jaramillo, T. F. *Nat. Mater.* **2012**, *11*, 963−969.